Available online at www.sciencedirect.com

SciVerse ScienceDirect

Ceramics International 39 (2013) 959–967

CERAMICS INTERNATIONAL

www.elsevier.com/locate/ceramint

Corrosion behavior of electrochemically assembled nanoporous titania for biomedical applications

K. Indira[a], U. Kamachi Mudali[b], N. Rajendran[a,*]

[a]Department of Chemistry, Anna University, Guinday Campus, Chennai, Tamilnadu 600025, India
[b]Corrosion Science and Technology Group, Indira Gandhi Center for Atomic Research, Kalpakkam, Tamilnadu 603102, India

Received 1 June 2012; received in revised form 4 July 2012; accepted 4 July 2012
Available online 27 July 2012

Abstract

Corrosion resistance of nanoporous titania was investigated in Hank's solution using potentiodynamic polarization and electrochemical impedance spectroscopic techniques. The phase structure, surface morphology and elemental composition of the untreated, anodized heat treated and anodized heat treated titanium specimens immersed in Hank's solution for seven days were characterized using X-ray diffraction, atomic force microscopy and scanning electron microscopy with energy dispersive X-ray spectroscopy techniques, respectively. The X-ray diffraction technique revealed that the anodized heat treated titanium exhibited anatase structure. The atomic force microscopic and scanning electron microscopic results showed that the titanium surface has transformed from a smooth to nanoporous surface depending on the anodization conditions. The energy dispersive X-ray spectroscopy results confirmed the formation of hydroxyapatite over the anodized titanium after immersion for seven days in Hank's solution. The electrochemical results revealed that the anodized heat treated titanium after seven day immersion in Hank's solution showed nobler shift in corrosion potential compared to untreated and anodized titanium. Hence, the results suggested that the nanoporous titania layer developed on titanium is a promising material for application as orthopaedic implants.

Keywords: B. X-ray methods; C. Impedance; D. TiO_2; E. Biomedical applications

1. Introduction

Titanium (Ti) metal and its alloys are widely used as dental and medical implant material due to their excellent biocompatibility, good corrosion resistance, durability and strength compared to other alloys such as 316 LSS and Co–Cr alloys [1–6]. These properties have been attributed to the natural oxide layer formed spontaneously on Ti surface. However, the surface being bio-inert results in the lack of bone bonding ability in the implant [7,8]. In order to enhance the bone bonding ability, the surface of the implant materials should be modified. Various surface treatments have been explored for producing Ti implants with enhanced biocompatibility. One among them is anodization, which induced the formation of rough and porous TiO_2 surfaces [9]. Presently anodization is one of the most commonly used methods to produce nanoporous surface due to its simplicity and feasibility. In addition, the size and shape of nanostructured materials can be tuned to the desire dimension.

Nanoporous structures are of significant importance in a variety of applications because they have certain common properties that are widely seen in nanomaterials [10]. In addition, they can also be used as templates to fabricate other nanostructure materials which further expand their potential applications. For implant materials, porosity is essential because it increases cellular adhesion and implant fixation. The porous structure allows the in-growth of body tissue, including bone tissue [11]. Titanium dioxide (TiO_2) with 3-d micro and nanoporous structures may enhance apatite forming ability when compared to dense TiO_2 layer [12]. In this view, corrosion resistance is one of the major requirements in the selection of a particular material for such a given application. It is well known that the hydroxyapatite coated materials showed good corrosion resistance in the implants [13]. Corrosion behavior on

*Corresponding author. Tel.: +91 44 2235 8659; fax: +91 44 2220 0660.
E-mail address: nrajendran@annauniv.edu (N. Rajendran).

0272-8842/$ - see front matter © 2012 Elsevier Ltd and Techna Group S.r.l. All rights reserved.
http://dx.doi.org/10.1016/j.ceramint.2012.07.013

bulk Ti and its alloys in ringer's solution [14], artificial saliva [15] and solutions containing fluoride or protein [16] has already been reported.

Therefore, in the present investigation, qualitative observation of the chemical anodization effects on the Ti surface in a mixture of 0.14 M hydrofluoric acid and 0.2 M glycerol electrolyte at 30 V for 1 h and the nucleation of hydroxyapatite on anodized Ti carried out using conventional methods such as X-ray diffraction techniques (XRD), atomic force microscopy (AFM) and scanning electron microscope (SEM) with energy dispersive X-ray spectroscope (EDX). In addition, the corrosion resistance of nanoporous titania layer developed on titanium was carried out using potentiodynamic polarization and electrochemical impedance spectroscopic techniques in Hank's solution.

2. Materials and methods

2.1. Sample preparation

Commercially pure Ti sheets (1.5 cm × 1.5 cm × 0.05 cm) obtained from M/s Ti anode fabricators Pvt. Ltd., Chennai, India were used for the anodization experiments. Highly pure analytical grade chemicals viz., hydrofluoric acid (HF, 40%), glycerol, sodium chloride (NaCl, 99.9%), potassium chloride (KCl, 99.8%), calcium chloride ($CaCl_2$, 98%), sodium hydrogen carbonate ($NaHCO_3$, 99.8%), di-sodium hydrogen orthophosphate (Na_2HPO_4, 99%), magnesium chloride hexahydrate ($MgCl_2 \cdot 6H_2O$, 99%), potassium di-hydrogen orthophosphate (KH_2PO_4, 99%), magnesium sulphate heptahydrate ($MgSO_4 \cdot 7H_2O$, 99.5%) and glucose were used for the present investigation. Deionized water was used for the preparation of electrolytes.

Prior to anodization, the surfaces of Ti samples were polished on both sides using silicon carbide paper up to 1000 grit. In order to produce a uniform and smooth surface, final polishing was done using alumina paste (1 μm size, obtained from M/s. Chennai Metco Pvt. Ltd., Chennai, India). The polished samples were then washed with soap solution, degreased with acetone and thoroughly rinsed with distilled water. These samples were then ultrasonicated in a mixture of acetone, 2-propanol and ethanol followed by pickling in a mixture of 0.9 M HF and 3.0 M HNO_3 for 1 min. Finally, the specimens were rinsed in distilled water and dried in air at room temperature.

2.2. Development of nanoporous titanium dioxide

Anodization was carried out using two electrode set up, Ti as the anode and Pt as the cathode. Both the electrodes were connected to a direct current (DC) voltage source (Aplab, Model L3230). All the experiments were carried out at room temperature using a mixture of 0.14 M HF and 0.2 M glycerol at 30 V for 1 h. The anodized samples were heat treated at 450 °C for 3 h at a heating and cooling rate of 30 °C per min. The vacuum of the furnace was maintained at 1×10^{-5} mbar during the heat treatment.

2.3. Electrolyte preparation

Hank's solution was prepared according to an earlier report [17]. In brief, the solution was prepared using the following chemicals viz., NaCl (8.00 g), KCl (0.40 g), $CaCl_2$ (0.18 g), $NaHCO_3$ (0.35 g), Na_2HPO_4 (0.48 g), $MgCl_2 \cdot 6H_2O$ (0.10 g), KH_2PO_4 (0.06 g), $MgSO_4 \cdot 7H_2O$ (0.10 g) and Glucose (1.00 g). All the chemicals were dissolved in that order in 1000 mL double distilled water, the temperature and pH were maintained at 37 °C and 7.4, respectively, under continuous magnetic stirring. In order to study the biocompatibility of the specimens, the anodized heat treated Ti samples were immersed in Hank's solution for 1 h and seven day.

2.4. Surface characterizations and wettability

X-ray diffraction (XRD) patterns of untreated, anodized heat treated and anodized heat treated Ti after seven day immersion in Hank's solution were obtained using STOE make diffractometer with Cu target (K_α, $\lambda = 1.54056$ Å). The surface topography of the samples was seen using Atomic Force Microscopy (AFM (NT-MDT SPM)) and the surface roughness was measured using AFM image analysis tools (NOVA Image Analysis software 1. 0. 26. 1443).The surface morphology of the samples was investigated using Scanning Electron Microscopy (SEM, Quanta 200) and the elemental composition of the specimens were analyzed using Energy Dispersive X-ray Spectroscopy (EDX) coupled with SEM.

The wettability of the specimens before and after anodization was observed using contact angle measurements. The contact angle subtended by water was measured using a contact angle meter (OCA 15EC, data physics instruments, Germany), the dosing volume and dosing rate were 10 μL and 1 μL/s, respectively.

2.5. Electrochemical characterization

Electrochemical experiments were performed using a conventional three-electrode cell assembly maintained at 37 °C. A saturated Ag/AgCl electrode was used as a reference electrode, a Pt sheet was used as the counter electrode and the test specimen (untreated, anodized heat treated Ti after 1 h and seven day immersion in Hank's solution) was used as the working electrode.

Potentiodynamic polarization experiments were carried out for untreated, anodized heat treated Ti after 1 h and 7 day immersion in Hank's solution using Solartron 1287 Electrochemical Interface. The electrode potential was anodically scanned at a scan rate of 10 mV min^{-1}. All the measurements were carried out in aerated and non stirred conditions. In order to obtain reliable results, the experiments were repeated in triplicate using Hank's

solution. The corrosion current density (I_{corr}) and corrosion potential (E_{corr}) of each sample were calculated from polarization curves with the help of Cview software.

The Electrochemical Impedance Spectroscopy (EIS) measurements were carried out using Solartron 1255 Frequency Response Analyzer (FRA) with Solartron 1287 electrochemical interface with the frequency ranging from 10^4 Hz to 10^{-2} Hz. The EIS measurements were represented in Bode Phase and Bode Impedance plots. For analysis of impedance data, the software program, Equivalent circuit was used which used a variety of electrical circuits to numerically fit the measured impedance data [18–21].

3. Results and discussion

3.1. XRD Studies

The XRD patterns of untreated, anodized heat treated and anodized heat treated Ti after seven days of immersion in Hank's solution, are given in Fig. 1. The XRD pattern of untreated Ti (Fig. 1a) showed the diffraction peaks at 2θ values of 35.2°, 38.3°, 40.2°, and 53.2° (JCPDS No: 44-1294), and the anodized heat treated Ti (Fig. 1b) exhibited the characteristic diffraction peaks of anatase phase of TiO_2 at 2θ values of 25.4° and 48.1° (JCPDS No: 21-1272) corresponding to the planes (1 0 1) and (2 0 0). This agreed well with the results of Park et al. [22]. The degree of crystallinity influences the dissolution and biological behaviour of hydroxyapatite, highly crystalline structures yield less dissolution to the coatings [23]. The XRD pattern of anodized heat treated Ti after seven days immersion in Hank's solution is shown in Fig. 1c, which indicated that the peaks corresponding to hydroxyapatite can be clearly detected (JCPDS No: 09-432). This result is in good agreement with the result of Xiao et al. [24].

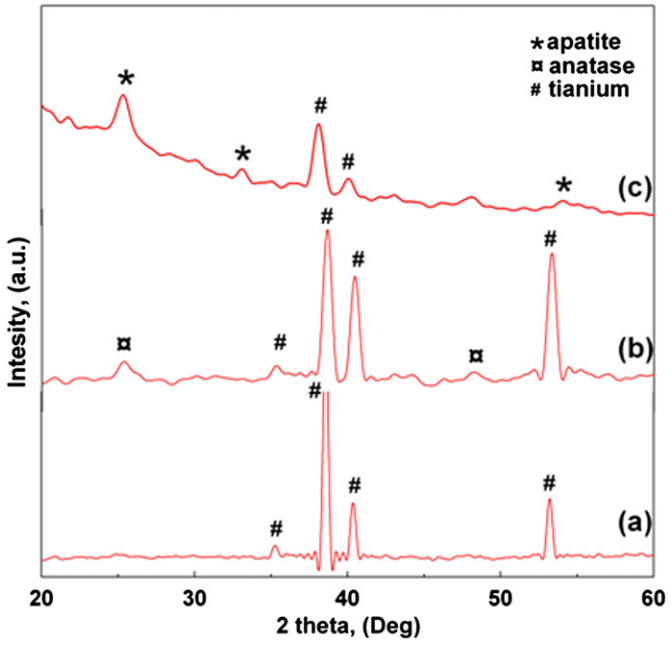

Fig. 1. XRD patterns of (a) untreated Ti and (b) anodized and heat treated Ti and (c) anodized Ti after seven day immersion in Hank's solution.

3.2. AFM studies

Fig. 2(a, c and e) shows the AFM topographs of anodized Ti and anodized Ti after immersion in Hank's solution for seven days in comparison to the untreated Ti surface and the corresponding line profile images are given in Fig. 2(b, d and f). The average surface roughness for the untreated and anodized Ti samples was found to be around 155 nm and 200 nm, respectively. The anodized samples immersed in Hank's solution exhibited the surface roughness of 186 nm. These results revealed that the roughness of the anodized heat treated Ti was higher than that of the untreated and anodized heat treated Ti immersed in Hank's solution. Anodization increased the surface roughness by forming a porous layer on Ti surface. The surface modified samples (anodized Ti) immersed in Hank's solution showed slightly lower surface roughness than the anodized Ti due to the deposition of Ca^{2+} and PO_4^{3-} ions in the Hank's solution on TiO_2 surface, which induces the formation of hydroxyapatite on the surface, thus decreasing the roughness of the surface [25]. Higher surface roughness provides early fixation and better mechanical stability for implants which resulted in good mechanical interlocking between the implant surface and bone in-growth [26]. It has been reported that a surface roughness of 10 nm to 10 μm can manipulate the interface biology [27]. Generally, biologically active implant materials have enhanced surface roughness, which was one of the important factors in providing better cell response to implanted materials [28].

3.3. SEM and EDX studies

Fig. 3(a, c and e) shows the SEM micrographs of anodized Ti and anodized Ti after immersion in Hank's solution for seven days in comparison to the untreated Ti surface. Visual observation of anodically formed TiO_2-films in a mixture of 0.14 M HF and 0.2 M glycerol showed different colors on the oxidized surfaces. This color change was mainly due to the change in thickness of the anodized Ti surface. It can be seen that after anodization, nanoporous structure was formed on the surface of Cp Ti.

The following processes occurred during anodization; initially the barrier oxide layer was formed at the metal/electrolyte interface which was then transformed into nanoporous layer due to the fluoride induced dissolution of the barrier oxide layer at the oxide/electrolyte interface [29], and pits were developed then subsequently changed into pores. Fluoride ion acts as an oxide layer dissolution agent [30].

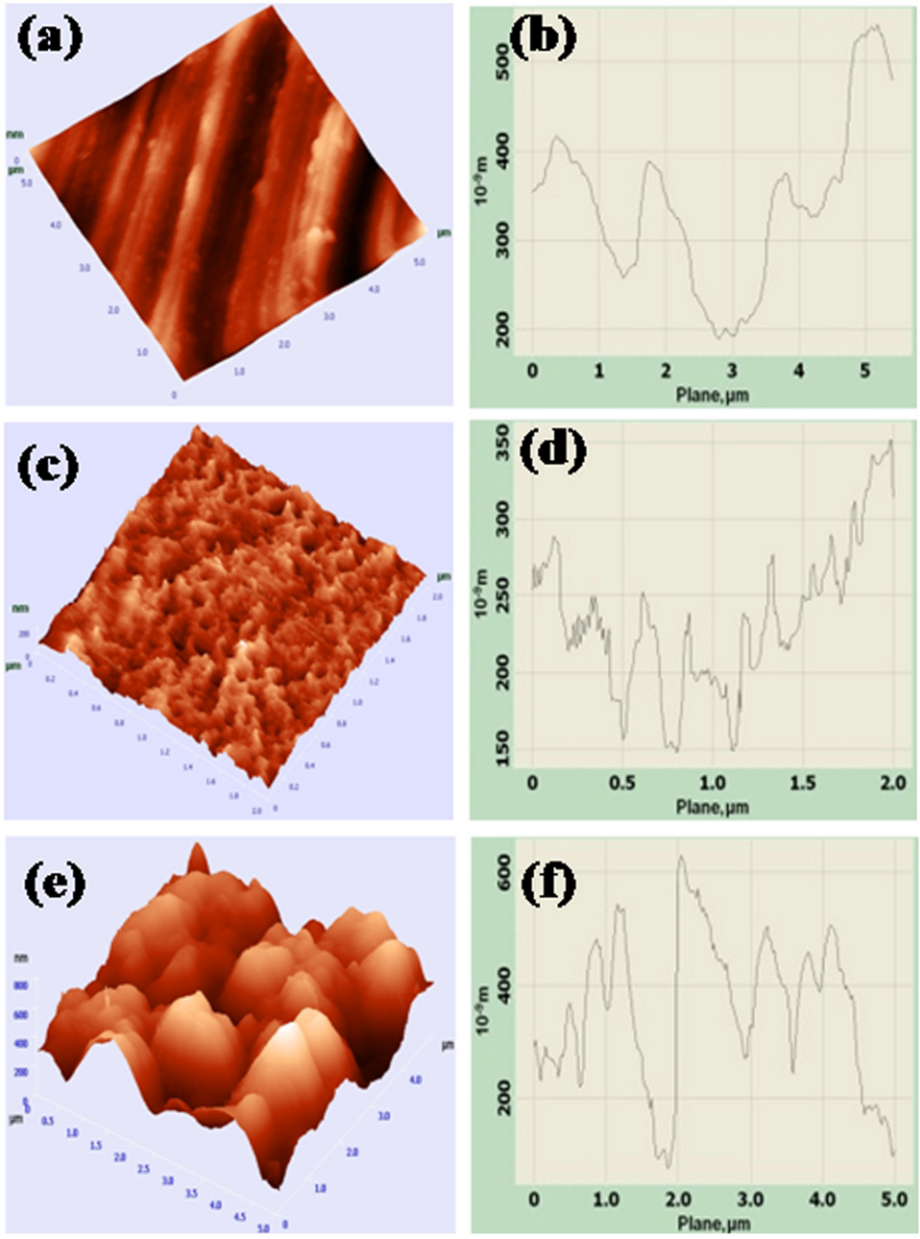

Fig. 2. AFM topographs of (a) untreated Ti, (c) anodized Ti and (e) anodized Ti after seven day immersion in Hank's solution and (b), (d) and (f) are the corresponding line profile images.

The porous film enhanced the hydroxyapatite formation which inhibits the dissolution of metal ions through the porous film, thus, enhancing the corrosion resistance [31]. It is well known that, calcium and phosphate ions present in physiological media interact with TiO_2 surfaces. By increasing the immersion time of the passivated metal in the simulated biological solutions, the formation of hydroxyapatite was found to increase on TiO_2 films [32].

Fig. 3(b, d and f) shows the EDX spectra of anodized Ti and anodized Ti after immersion in Hank's solution for seven days in comparison to the untreated Ti surface. The EDX results of untreated Ti showed major amount of Ti peaks and a small amount of oxygen peak which is due to the presence of native oxide layer whereas the anodized Ti contains Ti as well as O peaks which confirms the presence of (nanoporous, evidenced from Fig. 3c) the oxide layer. After seven days of immersion in Hank's solution, islands of apatite nuclei were seen on nanoporous titania surface under SEM observation, and the EDX spectrum showed the presence of Ca and P peaks which confirmed the formation of hydroxyapatite layer.

3.4. Wettability

The shape of water droplet was shown in Fig. 4. The contact angle values for untreated, anodized and anodized Ti after immersion in Hank's solution were found to be 86°, 125° and 64°, respectively. The wetting behavior of

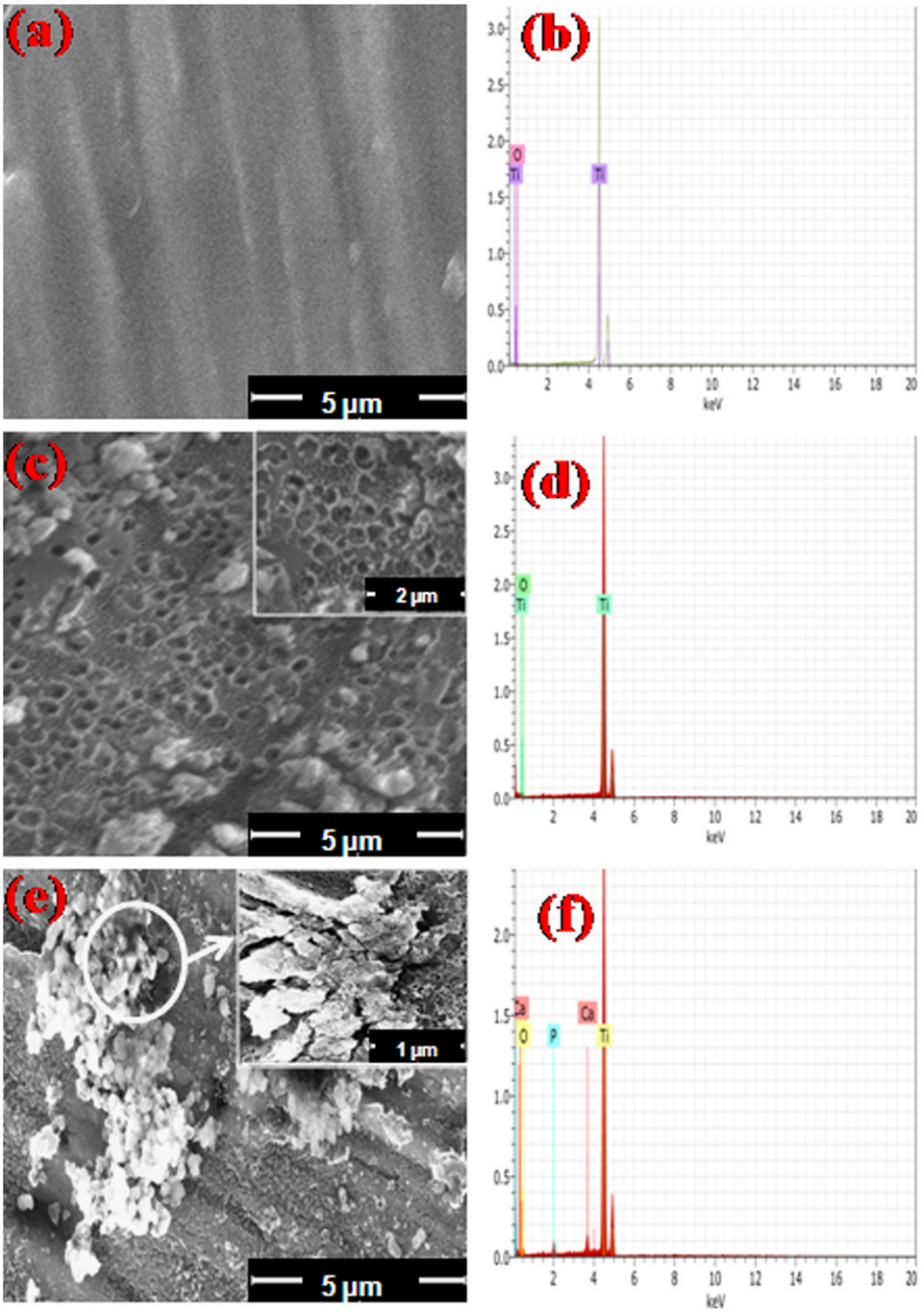

Fig. 3. SEM micrographs of (a) untreated Ti, (c) anodized Ti and (e) anodized Ti after seven day immersion in Hank's solution and EDX spectrum of (b) untreated Ti, (d) anodized Ti and (f) anodized heat treated Ti after seven day immersion in Hank's solution.

anodized Ti has improved greatly after immersion in Hank's solution by considerable decrease in contact angle. The anodized Ti after immersion in Hank's solution has hydrophilic property whereas the untreated and anodized Ti samples showed hydrophobic property with higher contact angle. The anodized Ti exhibited hydrophobic property as it has TiO_2 phase structure [33]. The Hank's solution spreads in an even way over the nanoporous titania surface making it less hydrophobic. Higher surface energy (lower contact angle) materials induced apatite formation.

3.5. Electrochemical characterization

3.5.1. Potentiodynamic polarization studies

Potentiodynamic polarization plots for untreated, anodized heat treated Ti after 1 h and seven day immersion in Hank's solution are shown in Fig. 5. The E_{corr} values of untreated Ti, anodized heat treated Ti after 1 h and seven day immersion in Hank's solution were found to be -1.03 V, -0.48 V and -0.42 V, respectively. It could be observed that the anodized Ti after seven days of immersion in Hank's solution exhibited higher E_{corr} and lower

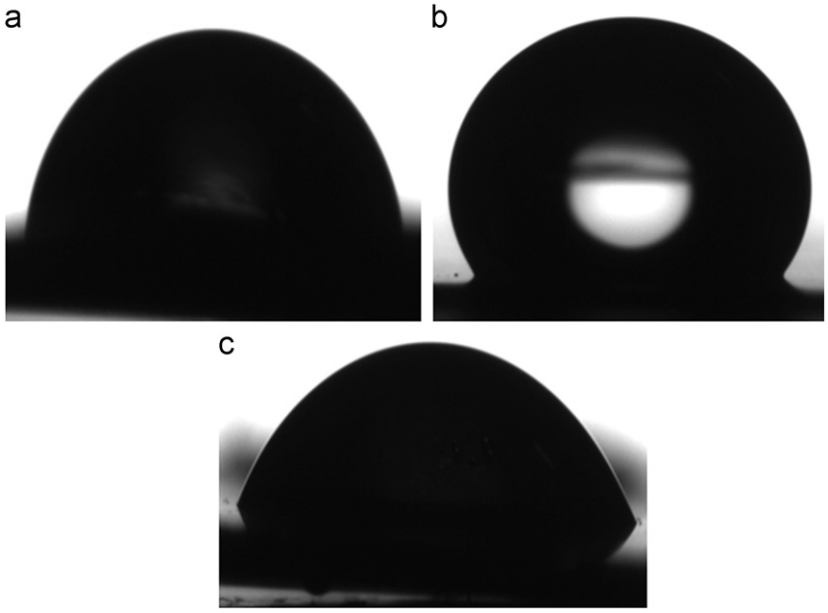

Fig. 4. Water droplet on (a) untreated Ti, (b) anodized Ti and (c) anodized Ti after seven day immersion in Hank's solution.

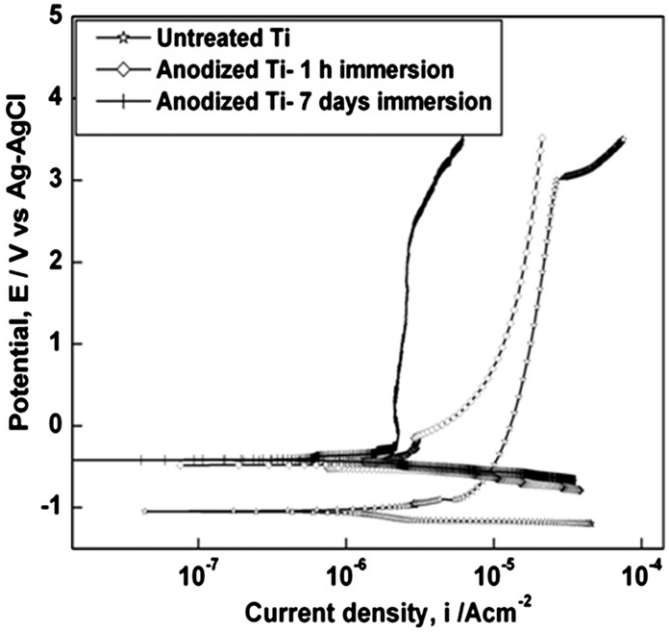

Fig. 5. Polarization curves of untreated Ti, anodized Ti after 1 h and seven day immersion in Hank's solution.

I_{corr} values when compared to untreated Ti and anodized Ti after 1 h immersion as shown in Table 1. Such an increase in potential for anodized Ti after seven days immersion in Hank's solution is attributed to the presence of hydroxyapatite on the anodized Ti surface.

Anodization provides a porous passive film which restricts the movements of metal ions from the metal surface to the solution [34]. The pores act perfectly as passive pits due to the higher barrier oxide thickness and compact pore walls. Therefore the effective surface area was increased for the nanopatterned surface and it gives the possible surface reaction [35]. Overall, the anodized Ti after seven day immersion in Hank's solution showed better corrosion resistance compared to the other samples.

Table 1
Polarization parameters of untreated Ti, anodized Ti after 1 h and seven day immersion in Hank's solution.

Specimen	$-E_{Corr}$ (Volts)	I_{Corr} (A cm^{-2})	R_p, (k Ω cm^2)
Untreated Ti	1.04	1.29×10^{-6}	20.05
Anodized Ti—1 h immersion	0.48	1.37×10^{-6}	20.40
Anodized Ti—seven day immersion	0.42	8.98×10^{-7}	67.93

3.5.2. Electrochemical impedance spectroscopic (EIS) studies

EIS was used to characterize the oxide films on Ti surface and to study the resistance of passive surface films [36]. EIS spectra of untreated, anodized heat treated Ti after 1 h and seven day immersion in Hank's solution are shown in Fig. 6. The Bode plots revealed that the spectra obtained for untreated Ti showed a phase angle value around -80° and remained constant over a wide range of frequencies, indicating highly capacitive behavior of the passive oxide film formed on its surface. The anodized Ti after seven day immersion in Hank's solution exhibited higher resistance compared to other samples which is due to the formation of a thick apatite layer on the surface.

Fig. 7 shows the equivalent circuit models which are obtained after fitting the spectra obtained from untreated, anodized heat treated Ti after 1 h and seven day immersion in Hank's solution. The fitted EIS results are tabulated in

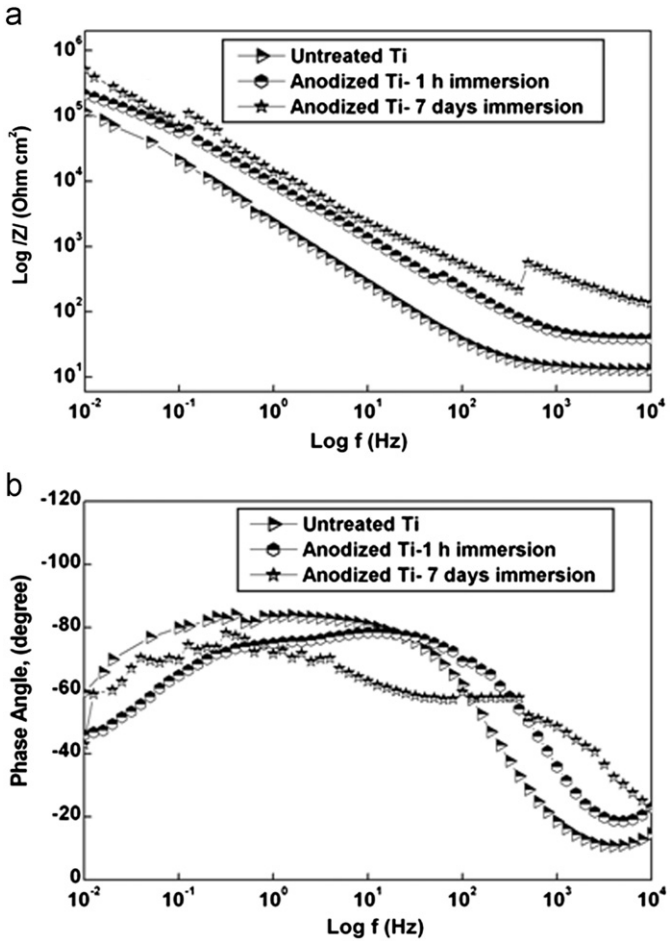

Fig. 6. (a) Bode phase angle and (b) Bode impedance plots of untreated Ti, anodized Ti after 1 h and seven day immersion in Hank's solution.

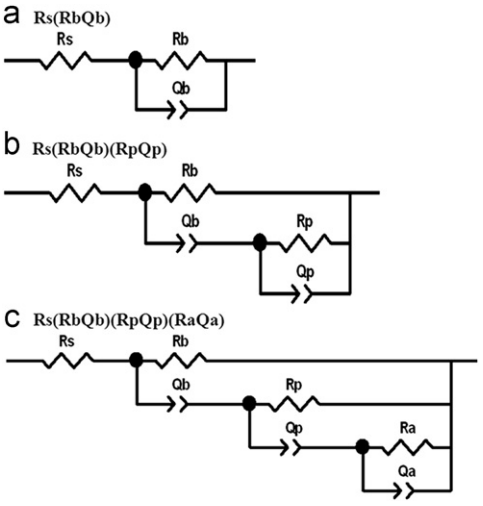

Fig. 7. Equivalent circuits used for (a) untreated Ti, (b) anodized Ti after 1 h immersion and (c) Anodized Ti after seven day immersion in Hank's solution.

Table 2. In order to characterize the passive oxide film on the untreated Ti, the EIS spectra was fitted with the model ($R_s(R_bQ_b)$) as shown in Fig. 7a, where R_s denotes the solution resistance, R_b is the polarization resistance of the barrier layer and Q_b is the double layer capacitance of the barrier layer. Instead of pure capacitance, Constant Phase Element (CPE) was introduced in the fitting to obtain good agreement between the simulated and experimental data. The impedance of CPE was defined by the Eq. (1) [37]

$$Z_{CPE} = [Q(j\omega)^n]^{-1} \quad (1)$$

where Q is the magnitude of CPE, ω is the angular frequency and n is the exponent of CPE with values between -1 and 1, which is related to non-uniform current distribution due to surface roughness [38]. It was observed that the untreated Ti exhibited only a single passive layer on its surface. From Table 1, the frequency independent parameter, n_b is 0.92 indicating a near capacitive behavior of the passive oxide film formed on untreated Ti. This suggested that the behavior of the surface layer approached that of an ideal capacitor [38].

The impedance spectrum was fitted and the model proposed for anodized Ti after 1 h immersion in Hank's solution is shown in Fig. 7b, where, R_b and R_p represent the polarization resistance of the barrier and porous layer, respectively. Q_b and Q_p are the double layer capacitance of the barrier and porous layer, respectively. The equivalent circuit showed two time constants which can be attributed to inner barrier and outer porous layers. The n_p value of the specimen was close to 1, which reveals that the porous layer behaved as an ideal capacitor. It has been reported that the outer porous layer exposed to the electrolyte contains anions from the solution and the inner layer is free of anions which is considered to be the barrier layer type ceramic [39].

Based on the EIS spectrum a three layer model (Fig. 7c) was used to interpret the obtained spectra for anodized Ti after seven day immersion in Hank's solution. In this model, R_b, R_p and R_a represent the polarization resistance of the barrier, porous and apatite layer, respectively. Q_b, Q_p and Q_a are the double layer capacitance of barrier, porous and apatite layer, respectively. The n_p and n_a values of the specimen were close to 1, which meant that the porous layer as well as the apatite layer behaved as an ideal capacitor. From the circuit parameters it was obvious that the polarization resistance of the porous layer greatly improved for anodized Ti after seven day immersion compared to that of the anodized Ti after immediate immersion, which has not been observed for untreated Ti. Apart from this, the capacitive value of the porous film was very low compared to anodized Ti after immediate immersion indicating the insulating property of the porous film. The high polarization resistance and low capacitance values indicated the existence of a superior protective layer on the surface.

When the Ti samples were immersed in Hank's solution, hydroxyapatite layer was formed [40]. The presence of third time constant after seven day immersion in Hank's solution is an indication that calcium and phosphate ions present in the Hank's solution interact and deposit on the surface. Similarly, Wang et al. [21] reported that nucleation and growth of bone-like apatite take place on chemically

Table 2
EIS spectra fitted values for untreated Ti, anodized Ti after 1 h and seven day immersion in Hank's solution.

Specimen	R_s (k Ω cm^2)	R_a (k Ω cm^2)	Q_a (F cm^{-2} S^n)	n_a	R_p (k Ω cm^2)	Q_p (F cm^{-2} S^n)	n_p	R_b (k Ω cm^2)	Q_b (F cm^{-2} S$^{n)}$	n_b
Untreated Ti	0.01	–	–	–	–	–	–	232.55	4.2×10^{-5}	0.92
Anodized Ti—1 h immersion	0.01	–	–	–	0.05	1.0×10^{-7}	0.99	396.09	2.9×10^{-6}	0.84
Anodized Ti—seven day immersion	0.01	0.14	1.0×10^{-7}	0.97	0.38	1.9×10^{-7}	0.96	1200.00	1.3×10^{-6}	0.80

R_s—solution resistance, R_b—polarization resistance of barrier layer, Q_b—double layer capacitance of barrier layer, R_p—polarization resistance of porous layer, Q_p—double layer capacitance of porous layer, R_a—polarization resistance of apatite layer and Q_a—double layer capacitance of apatite layer.

treated Ti surface on prolonged immersion in simulated body fluid solution.

From the above results, it can be confirmed that after seven day immersion in Hank's solution, the surface is covered with hydroxyapatite particles. The obtained results were also evidenced from EDX analysis (Fig. 3f). The anodized Ti after seven day immersion in Hanks solution showed the higher resistance and lower capacitance value. It is also can be evident that the anodized Ti exhibits higher corrosion resistance after seven day immersion in Hanks solution.

4. Conclusions

The nanoporous TiO_2 was developed by electrochemical anodization process using viscous organic electrolyte. The surface morphological studies of anodized Ti after seven days of immersion in Hank's solution showed the growth of bone-like apatite layer on its surface. The electrochemical studies indicated that the anodized Ti after seven days of immersion in Hank's solution exhibited very low corrosion current density and excellent corrosion resistance than those of anodized Ti after 1 h immersion and untreated Ti. Therefore, the anodized Ti is a suitable material for implantation in human body with high corrosion protection efficiency even after implantation.

Acknowledgements

The financial support provided by the University Grants Commission-Department of Atomic Energy (UGC-DAE) Consortium for Scientific Research is gratefully acknowledged. The authors also thank Mr. K. Thygarajan, CSTG, IGCAR, Kalpakkam for his help in heat treatment.

References

[1] U.Kamachi Mudali, T.M. Sridhar, Baldev Raj, Corrosion of bioimplants, Sadhana 28 (2003) 601–637.
[2] L. Thair, U. Kamachi Mudali, S. Rajagopalan, R. Asokamani, Baldev Raj, Surface characterization of passive film formed on nitrogen ion implanted Ti–6Al–4V and Ti–6Al–7Nb alloys using, SIMS Corrosion Science 45 (2003) 1951–1967.
[3] L. Thair, U. Kamachi Mudali, N. Bhuvaneswaran, K.G.M. Nair, R. Asokamani, B. Raj, Nitrogen ion implantation and in vitro corrosion behavior of as-cast Ti–6Al–7Nb alloy, Corrosion Science 44 (2002) 2439–2457.
[4] M. Geetha, U. Kamachi Mudali, A.K. Gogia, R. Asokamani, Baldev Raj, Influence of microstructure and alloying elements on corrosion behavior of Ti–13Nb–13Zr alloy, Corrosion Science 46 (2004) 877–892.
[5] A.W. Tan, B.P. Murphy, R. Ahmad, S.A. Akbar, Review of titania nanotubes: fabrication and cellular response, Ceramics International 38 (2012) 4421–4435.
[6] V. Kotharu, R. Nagumothu, C.B. Arumugam, M. Veerappan, S. Sankaran, M. Davoodbasha, T. Nooruddin, Fabrication of corrosion resistance, bioactive and antibacterial silver substituted hydroxyapatite/titania composite coating on Cp Ti, Ceramics International 38 (2012) 731–740.
[7] I.S. Park, T.G. Woo, W.Y. Jeon, H. Park, M.H. Lee, T.S. Bae, K.W. Seol, Surface characterization of titanium anodized in the four different types of electrolyte, Electrochimica Acta 53 (2007) 863–870.
[8] F. Liu, F. Wang, T. Shimizu, K. Igarashi, L. Zhao, Hydroxyapatite formation on oxide films containg Ca and P by hydrothermal treatment, Ceramics International 32 (2006) 527–531.
[9] A. Ghicov, P. Schmuki, Self-ordering electrochemistry: a review on growth and functionality of TiO_2 nanotubes and other self aligned MO_x structures, Chemical Communications (2009) 2791–2808.
[10] G. Wu, J. Zhang, X. Wang, J. Liao, H. Xia, S.A. Akbar, J. Li, S. Lin, X. Li, J. Wang, Hierarchical nanostructured TiO_2 nano-tubes for formaldehyde sensing, Ceramics International, (2012) http://dx.doi.org/10.1016/j.ceramint.2012.05.004.
[11] E.P. Banczek, S.L.D. Assis, M.V. Oliveira, W.S. Medeiros, L.C. Pereira, I. Costa, Corrosion resistance evaluation of porous titanium with biomimetic coatings, Materials Science Forum 591 (2008) 55–60.
[12] G.A. Crawford, N. Chawla, K. Das, S. Bose, A. Bandyopadhyay, Microstructure and deformation behavior of biocompatible TiO_2 nanotubes on titanium substrate, Acta Biomaterialia 3 (2007) 359–367.
[13] T.M. Sridhar, U. Kamachi Mudali, M. Subbaiyan, Preparation and characterization of electrophoretically deposited hydroxyapatite coating on type 316L stainless steel, Corrosion Science 45 (2003) 237–252.
[14] E.K. Cydzik, A. Kierzkowska, I. Glazowska, Behavior of anodic layer in Ringer's solution on Ti–6Al–4V ELI alloy after bending, Archives of Materials Science and Engineering 28 (2007) 231–237.
[15] V. Raman, S. Tamilselvi, S. Nanjundan, N. Rajendran, Electrochemical behavior of titanium and titanium alloy in artificial saliva, Trends in Biomaterials and Artificial Organs 18 (2005) 137–140.
[16] J.S. Chauhan, D.K. Gupta, Corrosion inhibition of titanium in acidic media containing fluoride with bixin, European Journal of Chemistry 6 (2009) 975–978.
[17] S. Tamil selvi, V. Raman, N. Rajendran, Corrosion behavior of Ti–6Al–7Nb and Ti–6Al–4V ELI alloys in simulated body fluid solution electrochemical impedance spectroscopy, Electrochimica Acta 52 (2006) 839–846.
[18] M. Aziz-Kerrzo, K.G. Conroy, A.M. Fenelon, S.T. Farrell, C.B. Breslin, Electrochemical studies on the stability and corrosion resistance of titanium based implant materials, Biomaterials 22 (2001) 1531–1539.
[19] S. Piazza, G.L. Biundo, M.C. Romano, C. Sunseri, F.D. Quarto, Insitu characterization of passive film on Al–Ti alloy by photocurrent and impedance spectroscopy, Corrosion Science 40 (1998) 1087–1108.

[20] M.J. Esplandiu, E.M. Patrito, V.A. Macagno, Characterization hafnium anodic oxide films: an AC impedance investigation, Electrochimica Acta 40 (1995) 809–815.
[21] C.X. Wang, M. Wang, Electrochemical impedance spectroscopy study of the nucleation and growth of apatite on chemically treated pure titanium, Materials Letters 54 (2002) 30–36.
[22] H.H. Park, I.S. Park, K.S. Kim, W.Y. Jeon, B.K. Park, H.S. Kim, T.S. Bae, M.H. Lee, Bioactive and electrochemical characterization of TiO_2 nanotubes on titanium via anodic oxidation, Electrochimica Acta 55 (2010) 6109–6114.
[23] N. Eliaz, T.M. Sridhar, U. Kamachi Mudali, Baldev Raj, Electrochemical and electrophoretic deposition of hydroxyapatite for orthopaedic applications, Surface Engineering 21 (2005) 1–5.
[24] X.F. Xiao, T. Tian, R.F. Liu, H.D. She, Influence of titania nanotube arrays on biomimetic deposition apatite on titanium by alkali treatment, Materials Chemistry and Physics 106 (2007) 27–32.
[25] S. Tamilselvi, V. Raman, N. Rajendran, Evaluation of corrosion behavior of surface modified Ti–6Al–4V ELI alloy in Hanks solution, Journal of Applied Electrochemistry 40 (2009) 285–293.
[26] L.L. Guehennec, A. Soueidan, P. Layrolle, Y. Amouriq, Surface treatments of titanium dental implants for osseointegration, Dental Materials 23 (2007) 844–854.
[27] C. Vasilescu, P. Drob, E. Vasilescu, I. Demetrescu, D. Ionita, M. Prodana, S.I. Drob, Characterisation and corrosion resistance of the electrodeposited hydroxyapatite and bovine serum albumin/hydroxyapatite films on Ti–6Al–4V–1Zr alloy surface, Corrosion Science 53 (2011) 992–999.
[28] K.S. Brammer, S. Oh, C.J. Frandsen, S. Jin, Biomaterials and biotechnology schemes utilizing TiO_2 nanotube arrays, Biomaterials Science and Engineering ISBN 978-953-307-609-6.
[29] X.Y. Fan, Y.H. Zhang, P. Xiao, F. Hu, H. Zhang, Chinese Journal of Chemical Physics 20 (2007) 753–758.
[30] B.G. Lee, J.W. Choi, S.E. Lee, Y.S. Jeong, H.J. Oh, C.S. Chi, Formation behavior of anodic TiO_2 nanotubes in fluoride containing electrolytes, Transactions of Nonferrous Metals Society of China 12 (2009) 842–845.
[31] A.M. Fekry, R.M.E. Sherif, Electrochemical corrosion behavior of magnesium and titanium alloys in simulated body fluid, Electrochimica Acta 54 (2009) 7280–7285.
[32] W.A. Badawy, A.M. Fathi, R.M.E. Sherief, S.A. Fadl-Allah, Electrochemical and biological behaviors of porous titania (TiO_2) in simulated body fluids for implantation in human bodies, Journal of Alloys and Compounds 475 (2009) 911–916.
[33] D.H. Shin, T. Shokuhfar, C.K. Choi, S.H. Lee, C. Friedrich, Wettability changes of TiO_2 nanotube surfaces, Nanotechnology 22 (2011) 315704.
[34] J. Baszkiewicz, D. Krupa, J. Mizera, J.W. Sobczak, A. Bilinski, Corrosion resistance of the surface layers formed on titanium by plasma electrolytic oxidation and hydrothermal treatment, Vacuum 78 (2005) 143–147.
[35] V.S. Saji, H.C. Choe, W.A. Brantley, An electrochemical study of self-ordered nanoporous and nanotubular oxide on Ti–35Nb–5Ta–7Zr alloy for biomedical applications, Acta Biomaterialia 5 (2009) 2303–2310.
[36] M.E.P. Souza, M. Ballester, C.M.A. Freire, EIS characterization of Ti anodic oxide porous films formed using modulated potential, Surface and Coatings Technology 201 (2007) 7775–7780.
[37] J. Liu, J. Yi, S. Li, M. Yu, G. Wu, L. Wu, Effect of electrolyte concentration on morphology, microstructure and electrochemical impedance of anodic oxide film on titanium alloy Ti–10V–2Fe–3Al, Journal of Applied Electrochemistry 40 (2010) 1545–1553.
[38] S. Tamil Selvi, N. Rajendran, In vitro corrosion behavior of Ti–5Al–2Nb–1Ta alloy in Hanks solution, Materials and Corrosion 58 (2007) 285–289.
[39] K. Lee, H.C. Choe, B.H. Kim, Y.M. Ko, The biocompatibility of HA thin films deposition on anodized titanium alloys, Surface and Coatings Technology 205 (2010) S267–S270.
[40] M. Karthega, N. Rajendran, Hydrogen peroxide treatment on Ti–6Al–4V alloy: a promising surface modification technique for orthopaedic application, Applied Surface Science 256 (2010) 2176–2183.